

## Theoretical Investigation of the Stereoselective Stepwise Cope Rearrangement of a 3-Vinylmethylenecyclobutane

Yi-Lei Zhao,<sup>†</sup> Christopher P. Suhrada, Michael E. Jung, and K. N. Houk\*

Contribution from the Department of Chemistry and Biochemistry, University of California, Los Angeles, California 90095-1569

Received February 16, 2006; E-mail: houk@chem.ucla.edu

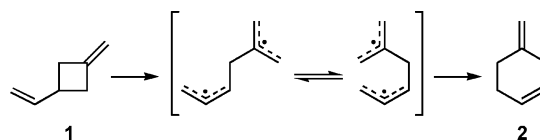
**Abstract:** The potential energy surface of the rearrangement of 3-vinylmethylenecyclobutane to 4-methylenecyclohexene has been studied computationally using density functional theory (B3LYP) and complete active space ab initio methods (CASSCF and CASPT2). The parent reaction is nonconcerted and occurs through several parallel diradical pathways. Transition structures and diradical intermediates are highly comparable in energy, with no deep potential energy well on the potential energy surface. In the substituted system, stereoelectronic effects of the trialkylsiloxy group regulate torquoselectivity in the bond-breaking processes and this, combined with low barriers to cyclization, leads to a stepwise Cope rearrangement that is, nevertheless, stereoselective.

Vinylcyclobutanes undergo a variety of thermal rearrangements and fragmentation reactions.<sup>1–3</sup> Most of these thermal reorganizations are of the “not obviously concerted” subclass<sup>1</sup> and do not obey Woodward–Hoffmann orbital symmetry rules. Because the activation energies for these reactions are comparable to bond dissociation energies, diradical mechanisms are generally accepted.<sup>3,4</sup>

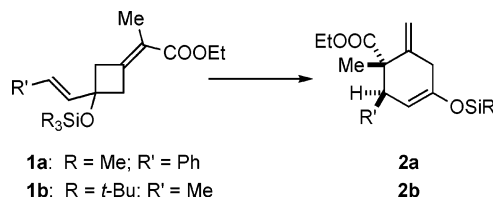
3-Vinylmethylenecyclobutanes have the possibility of undergoing both [1,3] and [3,3] shifts via either concerted or diradical mechanisms. The parent 3-vinylmethylenecyclobutane rearrangement (Scheme 1) has an experimental activation energy of 35.7 kcal/mol,<sup>5</sup> which is comparable to the energy expected for the homolysis of one of the endocyclic, doubly allylic C–C bonds. Deuterium-labeled derivatives rearrange in such a way as is expected for diradical intermediates, and considerable amounts of acyclic products were obtained in addition to [1,3]- and [3,3]-shift products.<sup>6</sup>

In contrast, the highly substituted 3-vinylmethylenecyclobutane **1a** was found to rearrange stereoselectively to form the Woodward–Hoffmann allowed [3s,3s]-sigmatropic shift product **2a** in greater than 90% yield (Scheme 2).<sup>7</sup> Upon replacement of the phenyl group with a methyl group, and TMSO with TBSO, the reaction (**1b** → **2b**) requires a higher temperature (135°C in a sealed tube) but still leads to only *cis*-(Me,Me) products, with the same overall stereochemistry.

**Scheme 1.** 3-Vinylmethylenecyclobutane-4-methylenecyclohexene Rearrangement



**Scheme 2.** Cope Rearrangements of **1** to **2** with Yields Greater than 90%



The [3s,3s]-sigmatropic rearrangements of **1a/b** to **2a/b** are analogous to the Cope rearrangement of 1,5-hexadiene, which has been studied thoroughly for decades.<sup>2,8</sup> The Cope rearrangement has the possibility of occurring in a single concerted step or through either a dissociative (bis-allyl) or associative (1,4-cyclohexanediyl) stepwise diradical mechanism.<sup>2,9</sup> For the parent 1,5-hexadiene, the concerted mechanism is well-established,<sup>2,10</sup> but radical-stabilizing substituents can divert the mechanism toward either of the possible diradical intermediates.<sup>9</sup>

<sup>†</sup> Present address: Computational Chemistry Group, NIST, Gaithersburg, MD 20899-8380.

- (1) Doering, W. v. E.; Cheng, X. H.; Lee, K.; Lin, Z. S. *J. Am. Chem. Soc.* **2002**, *124*, 11642.
- (2) Gajewski, J. J. *Hydrocarbon Thermal Isomerizations*, 2nd ed.; Elsevier Academic Press: Amsterdam, 2004.
- (3) Leber, P. A.; Baldwin, J. E. *Acc. Chem. Res.* **2002**, *35*, 279.
- (4) Suhrada, C. P.; Selçuk, C.; Nendel, M.; Cannizzaro, C.; Houk, K. N.; Rissing P.-J.; Baumann, D.; Hasselmann, D. *Angew. Chem., Int. Ed.* **2005**, *44*, 3548.
- (5) Dolbier, W. R.; Mancini, G. J. *Tetrahedron Lett.* **1975**, 2141.
- (6) Kozhushkov, S. I.; Kuznetsova, T. S.; Zefirov, N. S. *Dokl. Akad. Nauk SSSR* **1988**, *299*, 1395.
- (7) Jung, M. E.; Nishimura, N.; Novack, A. R. *J. Am. Chem. Soc.* **2005**, *127*, 11206.

- (8) (a) Borden, W. T.; Loncharich, R. J.; Houk, K. N. *Annu. Rev. Phys. Chem.* **1988**, *39*, 213. (b) Houk, K. N.; Li, Y.; Evanseck, J. D. *Angew. Chem., Int. Ed. Engl.* **1992**, *31*, 682. (c) Houk, K. N.; Gonzalez, J.; Li, Y. *Acc. Chem. Res.* **1995**, *28*, 81. (d) Borden, W. T.; Davidson, E. R. *Acc. Chem. Res.* **1996**, *29*, 67. (e) Wiest, O.; Montiel, D. C.; Houk, K. N. *J. Phys. Chem. A* **1997**, *101*, 8378.
- (9) Hrovat, D. A.; Chen, J.; Houk, K. N.; Borden, W. T. *J. Am. Chem. Soc.* **2000**, *122*, 7456.
- (10) (a) Hrovat, D. A.; Morokuma, K.; Borden, W. T. *J. Am. Chem. Soc.* **1994**, *116*, 1072. (b) Weist, O.; Black, K. A.; Houk, K. N. *J. Am. Chem. Soc.* **1994**, *116*, 10336. (c) Kozłowski, P. M.; Dupuis, M.; Davidson, E. R. *J. Am. Chem. Soc.* **1995**, *117*, 774. (d) Jiao, H.; Schleyer, P. v. R. *Angew. Chem., Int. Ed. Engl.* **1995**, *34*, 334. (e) Staroverov, V. N.; Davidson, E. R. *J. Am. Chem. Soc.* **2000**, *122*, 186.

**Scheme 3.** 3-Vinylmethylenecyclobutane Rearrangement of 6-Methylenebicyclo[3.2.0]hept-2-ene



Additionally, geometric constraints may favor a dissociative stepwise mechanism, especially where ring strain lowers the homolysis energy for the initial bond scission step. Such is the case in the bicyclic 3-vinylmethylenecyclobutane rearrangement studied by Hasselmann et al. (Scheme 3), which leads to both [3,3]- and [1,3]-shift products in a stepwise manner.<sup>4</sup>

With this background in mind, we report a theoretical study of the parent 3-vinylmethylenecyclobutane rearrangement, as well as substituted models for the stereoselective rearrangement of **1a/b** to **2a/b**, to determine the nature of the mechanism, the effects of substituents, and the cause of the observed stereoselectivity.

### Computational Methodology

Stationary point structures were optimized using (U)B3LYP/6-31+G(d) and (6,6)CASSCF/6-31+G(d) in Gaussian 03<sup>11</sup> and Gaussian 98<sup>12</sup> (substituted model systems were optimized with UB3LYP only). In the unrestricted DFT calculations, Guess = Mix and Guess = (Mix, Always) were used to avoid artifactual restricted solutions with unstable wave functions. Vibrational frequency analyses were carried out on all optimized structures to confirm their nature as minima or first-order saddle points. UB3LYP zero-point and thermal corrections (unscaled frequencies at 383 K and 1 atm) have been applied throughout, even to CASSCF-optimized structures, for uniformity. (6,6)CASPT2/6-31G(d) single-point energy calculations were conducted with MOLCAS 5.0<sup>13</sup> on both UB3LYP- and CASSCF-optimized geometries. These methods have been found to give reasonable energies for similar diradical and pericyclic processes.<sup>14</sup>

### Results and Discussion

**Rearrangement of the Parent System.** When RB3LYP/6-31+G(d) was used, it was possible to locate a concerted [3s,3s] transition structure for the 3-vinylmethylenecyclobutane rearrangement (**TS-1-2**, see Supporting Information). **TS-1-2** is a distorted, chairlike transition structure with long breaking and forming C–C bonds (2.2 and 2.8 Å, respectively). However, both UB3LYP and CASSCF calculations indicate that this saddle point is only an artifact of the restricted formalism and that all minimum-energy pathways from **1** to **2** involve an intermediate diradical minimum.

UB3LYP and CASSCF results were very similar to each other; the following discussion and the accompanying figures employ UB3LYP/6-31+G(d)-optimized structures and CASPT2/6-31G(d)//UB3LYP/6-31+G(d) relative enthalpies.

There are four modes of C3–C6<sup>15</sup> cleavage leading to diradical intermediates (Figure 1). Generally, these bond-breaking transition structures are characterized by the lengthening of C3–C6 and simultaneous twisting of C6 and its substituents into conjugation with the C5–C7  $\pi$  bond. **TS-1-3**

and **TS-1-4** form a diradical with a *trans*-C1–C2–C3 allyl unit (**3** or **4**), while **TS-1-5** and **TS-1-6** form C1–C2–C3 *cis*-intermediates. Because the *trans*-configuration of **3** and **4** prevents ring-enlarging formation of a new bond to C1, **3** and **4** cannot proceed to **2** and can only revert to **1**. Accordingly, these pathways are unproductive and can serve only to rearrange labeling substituents in the educt **1**. Thermal interconversion between *trans*- and *cis*-intermediates (**3** or **4**  $\rightleftharpoons$  **5** or **6**) is estimated to have a barrier of approximately 16 kcal/mol<sup>4,16</sup> and, therefore, is expected not to occur within the lifetime of the intermediates.

Among the transition structures that *can* ultimately lead to **2**, **TS-1-5** is favored over **TS-1-6** by about 0.5 kcal/mol. In **TS-1-5**, C3–C6 bond cleavage is accompanied by twisting of the four-membered ring toward more negative values of D(3,4,5,6) as drawn in Figure 1. The vinyl group meanwhile rotates outward to occupy an equatorial-like position on the breaking four-membered ring. This motion ultimately results in the extended conformation of the diradical **5**. Meanwhile, the substituents on C6 twist in the same sense as those at C3 (counterclockwise in the figure), reminiscent of a conrotatory electrocyclic ring opening, leaving Hx *trans* to C4 on the C6–C5–C7 allyl unit. In **TS-1-6**, which is less-favored, the breaking ring twists in the opposite direction (toward positive D(3,4,5,6)) and the vinyl substituent rotates into an axial-like position—toward the breaking ring rather than away from it. The reaction coordinate is characterized by decreasing values of D(2,3,4,5) until this motion is arrested near the metastable diradical structure **6** as a result of its unfavorable steric implications. Like **TS-1-5**, **TS-1-6** involves a kind of conrotatory twisting at C3 and C6, only in the opposite direction, leaving Hx in a position *cis* to C4. **TS-1-5** and **TS-1-6** closely resemble the respective favored and disfavored bond-breaking transition structures found for Hasselmann's 6-methylenebicyclo [3.1.0] hept-2-ene rearrangement.<sup>4</sup> In the nomenclature introduced in that communication, **TS-1-5** would be an “endo” transition state, so-called because C6 appears to move inward, across the C1–C2  $\pi$  bond, as it departs from C3. Likewise, **TS-1-6** is an “exo” transition state because C6 leaves C3 on the side away from C1–C2. The preference for **TS-1-5** changes with the introduction of a trialkylsiloxy group at C3, as will be discussed in a subsequent section of this report.

Beyond the 34.9 and 35.4 kcal/mol barriers at **TS-1-5** and **TS-1-6**, diradical intermediates reside in a broad, shallow potential energy well with a range of 30.0–32.0 kcal/mol relative to **1**. On the UB3LYP electronic energy surface (Figure 2), the C<sub>s</sub> symmetric structure **5** is actually a saddle point representing an extremely small barrier between two nonsymmetric flanking structures **5a**. Because the energy difference between **5** and **5a** is entirely insignificant, we will consider them as constituting a single potential energy minimum for an “extended” diradical conformation. The “compact” diradical structure **6**, which connects directly to **TS-1-6**, and to the bond-forming transition states **TS-6-2-n** and **TS-6-2-x** on the UB3LYP and CASSCF surfaces, appears to be a metastable conformer at best, being separated from the principal well **5** by a barrier that ranges from 1.6 kcal/mol according to CASPT2//CASSCF to nil by CASPT2//UB3LYP. Whether or not it is technically a

(11) Frisch, M. J. et al. *Gaussian 03*, revision C.02.; Gaussian, Inc.: Wallingford, CT, 2004.

(12) Frisch, M. J. et al. *Gaussian 98*, revision A.9.; Gaussian, Inc.: Pittsburgh, PA, 1998.

(13) Andersson, K. et al. *Molcas*, version 5.0.; Lund University: Sweden, 2001.

(14) Guner, V.; Khuong, K. S.; Leach, A. G.; Lee, P. S.; Bartberger, M. D.; Houk, K. N. *J. Phys. Chem. A* **2003**, *107*, 11445.

(15) For the sake of consistency and simplicity, we will use the atom numbering system introduced in Figure 1, rather than the standard IUPAC numbering for the reactant or product, throughout the Results and Discussion section.

(16) Korth, H. G.; Trill, H.; Sustmann, R. *J. Am. Chem. Soc.* **1981**, *103*, 4483.

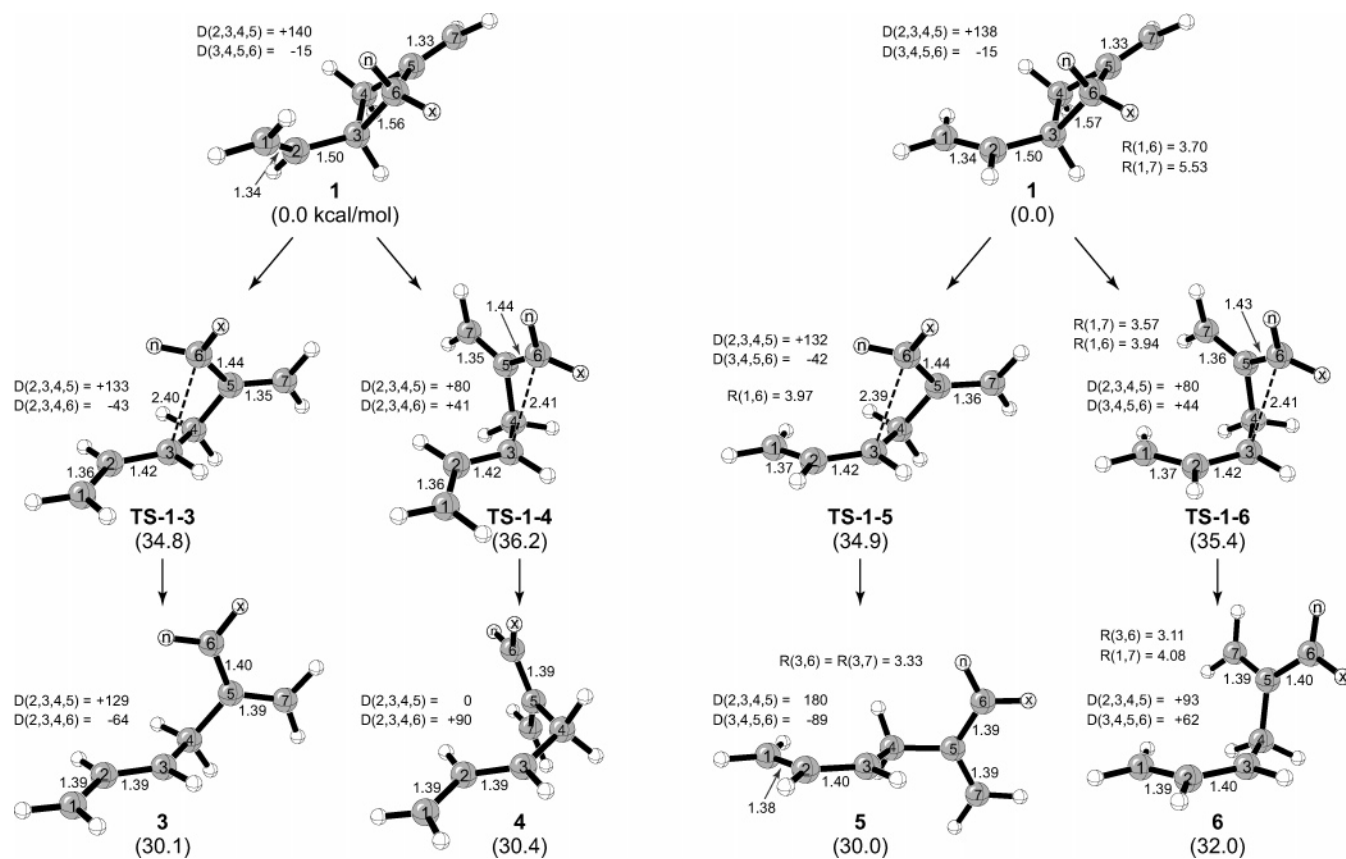


**Figure 1.** Four transition states for bond breaking lead to bis-allyl diradical intermediates. UB3LYP/6-31+G(d)-optimized structures are shown with (6,6)-CASPT2/6-31G(d)//UB3LYP/6-31+G(d) enthalpies listed in kcal/mol relative to **1**. Selected bond distances (angstroms) and dihedral angles (degrees) are listed for each structure.

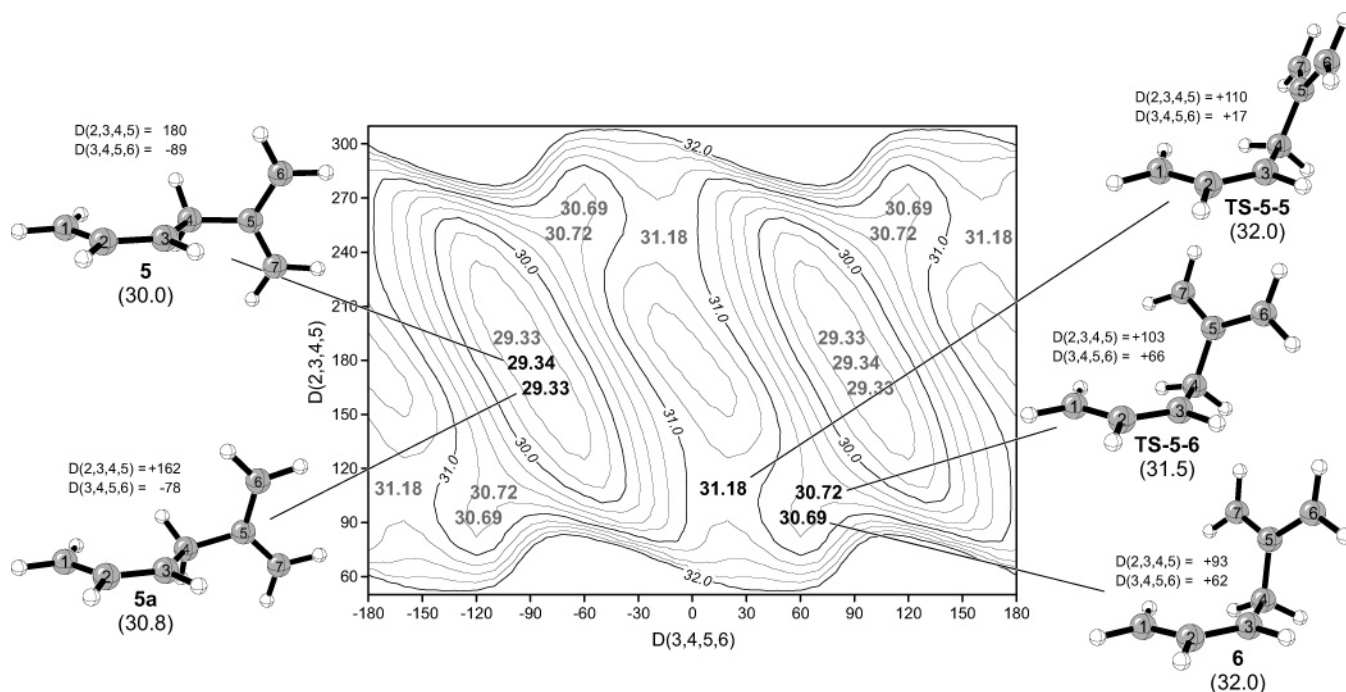


**Figure 2.** Electronic potential energy surface for C1–C2–C3 cisoid diradical species, generated by UB3LYP/6-31+G(d) optimizations constrained in the dihedral coordinates  $D(2,3,4,5)$  and  $D(3,4,5,6)$ . Energy contours and stationary point positions on the plot are labeled as electronic energy in kcal/mol relative to **1**. UB3LYP/6-31+G(d)-optimized stationary point structures are shown with their CASPT2//UB3LYP enthalpies (in parentheses; kcal/mol relative to **1**).

distinct minimum is not terribly important, however; **6** may be thought of as merely an easily accessible “reactive” diradical conformation. Each  $C_s$  minimum **5** connects to two reactive

conformers **6** via rotation about  $D(2,3,4,5)$ . Transition states **TS-5-5** at 2.0 kcal/mol above the diradical minimum **5** mediate  $D(3,4,5,6)$  rotation.

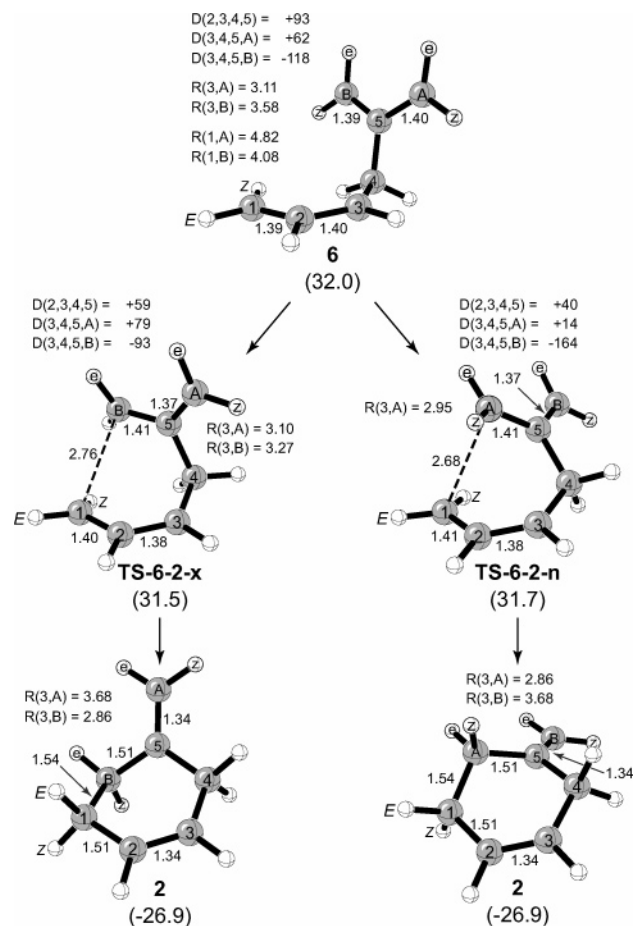


**Figure 3.** UB3LYP/6-31+G(d) transition structures for cyclization of diradical intermediate to isomeric 4-methylenecyclohexanes, **2**. (6,6)-CASPT2/6-31G(d)//UB3LYP/6-31+G(d) enthalpies are listed in kcal/mol relative to **1**, along with selected bond distances (angstroms) and dihedral angles (degrees).

From the diradical, ring-expansion is completed by the formation of a new bond to C1. Similar to the bond-breaking step, there are two stereoisomeric alternatives (Figure 3). The more distant allyl terminus CA can pass over C3 and C2 to form a bond to C1—an “endo” approach—in which case CA-*e* and C1-*E* substituents are left *trans* to each other on the six-membered ring (TS-6-2-*n*). Alternatively, TS-6-2-*x* forms a new bond from CB to C1 via an “exo” approach, placing the “*e*” substituent on CB *cis* to the *E* substituent on C1. Both transition states are characterized by very long forming bond distances. A very small energy difference (0.2 kcal/mol) favors TS-6-2-*x*.

According to CASPT2//UB3LYP, TS-6-2-*x* and TS-6-2-*n* lie only 1.5 and 1.7 kcal/mol above **5**. This is slightly lower than the isomerization barrier TS-5-5 and even diradical conformer **6** (both 2.0 kcal/mol above **5**). In fact, considering all of the

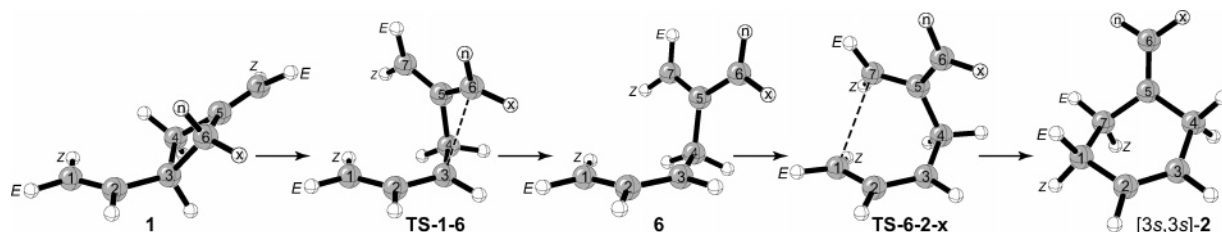


**Figure 4.** Stepwise reaction path producing a formal [3s,3s] Cope rearrangement.

**Table 1.** Calculated Relative Enthalpies for Stationary Points in the Rearrangement of 3-Vinylmethylenecyclobutane (**1**) to 4-Methylenecyclohexene (**2**) from (U)B3LYP/6-31+G(d) and (6,6)CASSCF/6-31+G(d) Optimizations, as Well as (6,6)CASPT2/6-31G(d) Single-Point Energy Calculations on Both Sets of Structures<sup>a</sup>

|                  | UB3LYP | CASPT2//UB3LYP | CASSCF | CASPT2//CASSCF |
|------------------|--------|----------------|--------|----------------|
| <b>1</b>         | 0.0    | 0.0            | 0.0    | 0.0            |
| <b>2</b>         | -24.8  | -26.9          | -31.0  | -25.9          |
| TS-1-3           | 35.2   | 34.8           | 33.4   | 36.6           |
| TS-1-4           | 37.0   | 36.2           | 34.9   | 38.1           |
| <b>3</b>         | 26.3   | 30.1           | 26.0   | 31.1           |
| <b>4</b>         | 27.2   | 30.4           | 27.5   | 31.4           |
| TS-1-5           | 35.2   | 34.9           | 33.4   | 36.7           |
| TS-1-6           | 36.5   | 35.4           | 34.8   | 37.7           |
| <b>5</b>         | 26.3   | 30.0           | 25.9   | 31.0           |
| <b>6</b>         | 28.6   | 32.0           | 28.2   | 32.8           |
| TS-6-2- <i>x</i> | 32.6   | 31.5           | 32.9   | 33.3           |
| TS-6-2- <i>n</i> | 32.2   | 31.7           | 32.4   | 33.5           |
| TS-5-6           | 27.8   | 31.5           | 27.6   | 32.6           |
| TS-5-5           | 28.2   | 32.0           | 28.1   | 32.9           |

<sup>a</sup> UB3LYP/6-31+G(d) thermal corrections to enthalpy (383 K, 1.0 atm, frequencies unscaled) have been applied uniformly throughout for consistency.

energetics revealed for the parent vinylmethylenecyclobutane reaction (Table 1), it is difficult to define rigorously all the relevant minima, transition structures, and intervening minimum-energy paths for the rearrangement of **1** to **2**. It appears appropriate to conclude simply that diradical intermediates formed from **1** via TS-1-5 and TS-1-6 have substantial conformational freedom and very low barriers for forming stereo- and regioisomeric forms of the ring-enlarged product **2**. This model is consistent with the small amount of experimental data that exist for the parent reaction: deuterium labeling experiments thus far<sup>6</sup> offer no stereochemical data, but they do show an absence of regioselectivity between [1,3] and [3,3] shifts, as well as several acyclic products, likely resulting from diradicals **3** and **4**. The calculations reported here also reasonably reproduce the experimentally determined activation energy of 35.7 kcal/mol.<sup>5</sup>

Within the theoretical framework developed here, a formal [3s,3s] Cope rearrangement could be achieved by following a path from **1** through TS-1-6, then immediately cyclizing from diradical conformer **6** via TS-6-2-*x* (Figure 4). For this pathway to be favored, TS-1-6 would have to predominate over TS-1-5, and the intermediate diradical would have to undergo cyclization in its initial conformation before it could isomerize, either for dynamic reasons or simply because cyclization barriers were lower than those to conformational rearrangement. For the parent system, calculations predict and experiments demonstrate that this path is not favored significantly over others.

In contrast to the nonselective parent system, however, the substituted systems studied by Jung et al.<sup>7</sup> show a high degree of selectivity. It is clear that the introduction of substituents

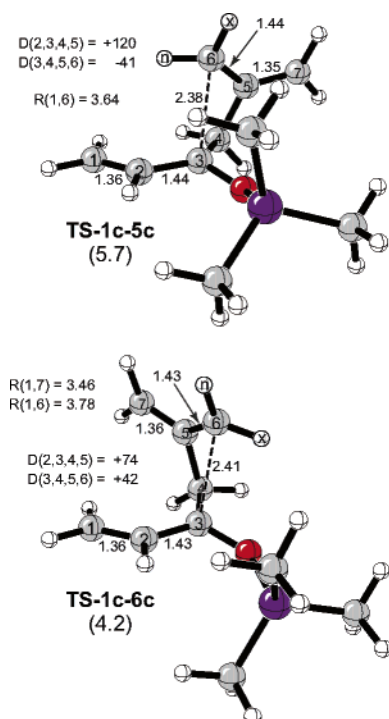


**Figure 5.** UB3LYP/6-31+G(d)-optimized transition structures for ring-opening from 3-trimethylsiloxy-1 (**1c**, not shown). Selected bond distances (angstroms) and dihedral angles (degrees) are listed on the figure; CASPT2//UB3LYP enthalpies in kcal/mol relative to **6c** (Figure 7) are shown in parentheses.

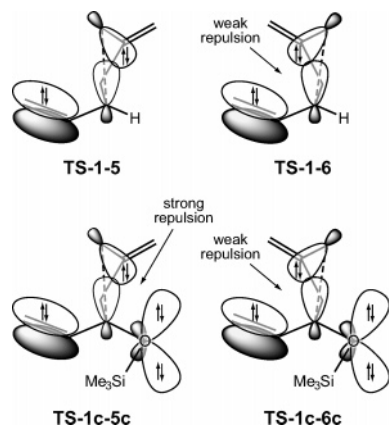


**Figure 6.** Schematic representation of the filled-orbital interactions influencing **TS-1-5** versus **TS-1-6** preferences.

must change the profile of the reaction substantially. The following sections describe calculations on partially substituted model systems to determine the factors that influence selectivity.

#### Trialkylsiloxy Substitution Effects on Bond Cleavage.

Figure 5 shows the siloxy effect on the ring-opening process. Dramatically, siloxy substitution reverses the **TS-1-5**/**TS-1-6** preference found in the parent system. **TS-1c-5c** is actually 1.5 kcal/mol higher in enthalpy than **TS-1c-6c**, according to (6,6)-CASPT2/6-31G(d)//UB3LYP/6-31+G(d). The reversal from 0.5 kcal/mol in favor of **TS-1-5** to 1.5 kcal/mol in favor of **TS-1c-6c** amounts to a 2.0 kcal/mol penalty imposed upon the “endo” transition state by the trialkylsiloxy group. As described above, enhancement of **TS-1-6** relative to **TS-1-5** could be crucial to favoring the [3s,3s] Cope-like product.

Inversion of the **TS-1-5**/**TS-1-6** preference by the siloxy group is likely related to the torquoselectivity characteristics of alkoxy

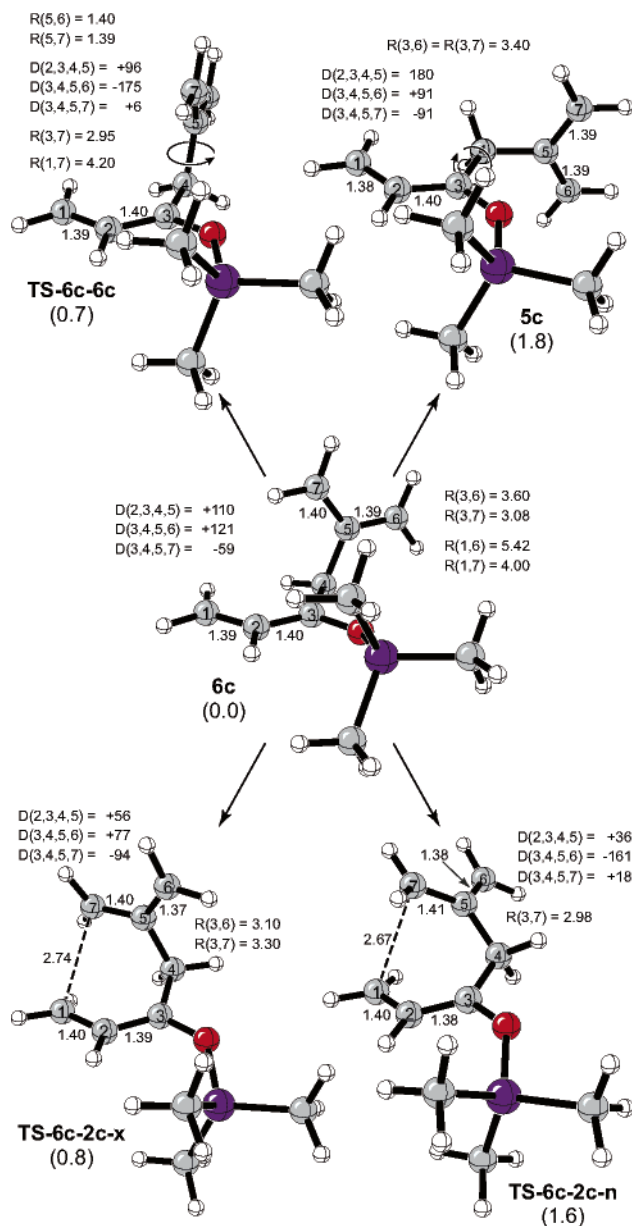


**Figure 7.** UB3LYP/6-31+G(d)-optimized diradical intermediate **6c** with transition structures for diradical isomerization (**5c** and **TS-6c-6c**) and for product formation (**TS-6c-2c-n** and **TS-6c-2c-x**). Selected bond distances (angstroms) and dihedral angles (degrees) are listed on the figure; CASPT2//UB3LYP enthalpies in kcal/mol relative to **6c** are shown in parentheses.

groups in cyclobutene electrocyclic ring openings.<sup>17</sup> Whereas in the parent **TS-1-5**, the electron density of the breaking C3–C6  $\sigma$  bond faces away from that of the vinyl  $\pi$  bond, in **TS-1c-5c** there is unfavorable overlap between the breaking C3–C6  $\sigma$  and the lone-pair orbitals on oxygen. **TS-1c-6c** avoids this  $\sigma$ -lone-pair repulsion at the apparently lesser expense of the  $\sigma$ - $\pi_{\text{vinyl}}$  repulsion that makes **TS-1-6** less-favorable in the unsubstituted case (Figure 6). This is in good agreement with the much larger outward torquoselectivity preference calculated for alkoxy versus vinyl substituents in cyclobutene.<sup>17</sup>

#### Siloxy Substitution Effects on Diradical Conformation.

The data for the parent system in Figure 2 indicate that energetics favor the highly symmetric structures **5** over the more

(17) Dolbier, W. R.; Koroniak, H.; Houk, K. N.; Sheu, C. M. *Acc. Chem. Res.* **1996**, *29*, 471.

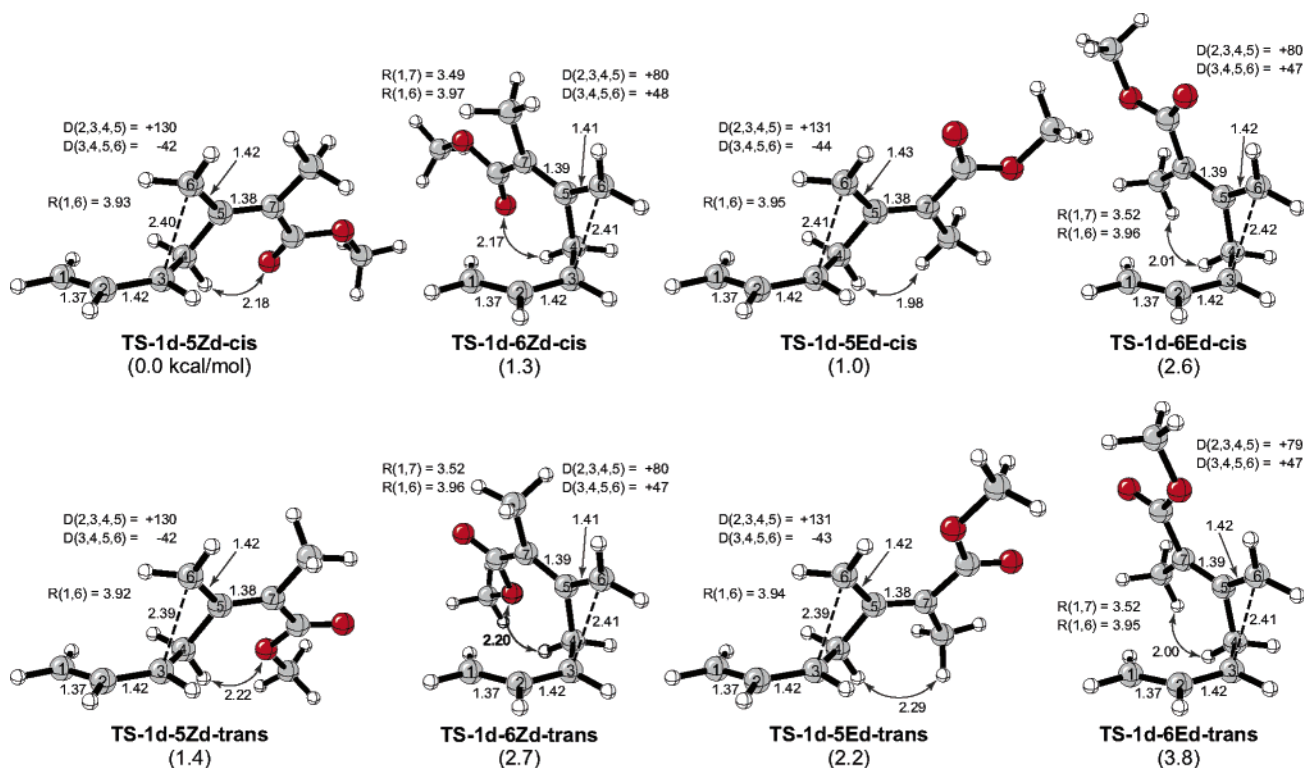


**Figure 8.** UB3LYP/6-31+G(d)-optimized transition structures for C3–C6 bond cleavage from 7-methyl-7-(methoxycarbonyl)-1 (**1d**, Scheme 4). UB3LYP/6-31+G(d) relative enthalpies are listed in kcal/mol relative to **TS-1d-5Zd-cis**.

stereochemically differentiated structures **6**. Thus, a diradical formed from **1** via **TS-1-5** or **TS-1-6** will quickly lose much of its initial stereochemical identity. Model calculations show that this situation may change upon OSiR<sub>3</sub> substitution at C3 (Figure 7). The planar structure **5c** is found to be a transition state for D(2,3,4,5) rotation, straddled by nonsymmetric structures **6c**. As opposed to the more symmetric **5c**, **6c** would retain full stereochemical “memory” of its formation (from **TS-1c-6c** or **TS-1c-5c**), thereby affecting the regio- and stereochemistry of the product. This change in the diradical potential surface would help to fulfill the requirement for apparent Cope rearrangement that diradical intermediates resulting from **TS-1-6** do not conformationally rearrange before undergoing cyclization.

**Ester and Methyl Group Effects on Bond Cleavage.** Substitution on the methylene by an ester group (COOMe) and a methyl group (Me) multiplies the stereochemical possibilities for the bond-breaking step. Namely, the two endocyclic bonds to C3 become nonequivalent, as cleavage can occur either at the bond nearer to Me or at the bond nearer to COOMe. This multiplies the two transition structures **TS-1-5** and **TS-1-6** to four. Additionally, the ester group may adopt two different conformations with respect to rotation about the bond C7–COOMe, with the carbonyl either *s-cis* or *s-trans* to C5. All together, there are eight transition structures for productive bond cleavage; these are shown in Figure 8. *s-cis*-Carbonyl rotamers are generally favored by 1.2–1.4 kcal/mol over their *s-trans* counterparts. **TS-1d-6ds** lie 1.3–1.6 kcal/mol higher in energy than the corresponding **TS-1d-5ds**, similar to UB3LYP/6-31+G(d) estimates for the parent system. Most importantly, we find a preference of 1.0–1.4 kcal/mol for cleavage of the cyclobutane bond nearer to Me, resulting in diradicals with a *Z* configuration about C5–C7. While the carbonyl O and C4–H may actually have an attractive interaction in these so-called “*Z*” transition

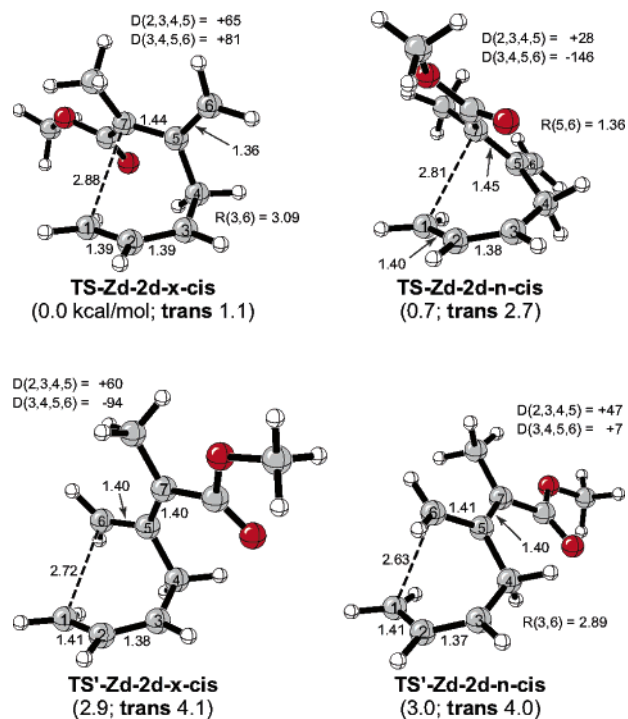
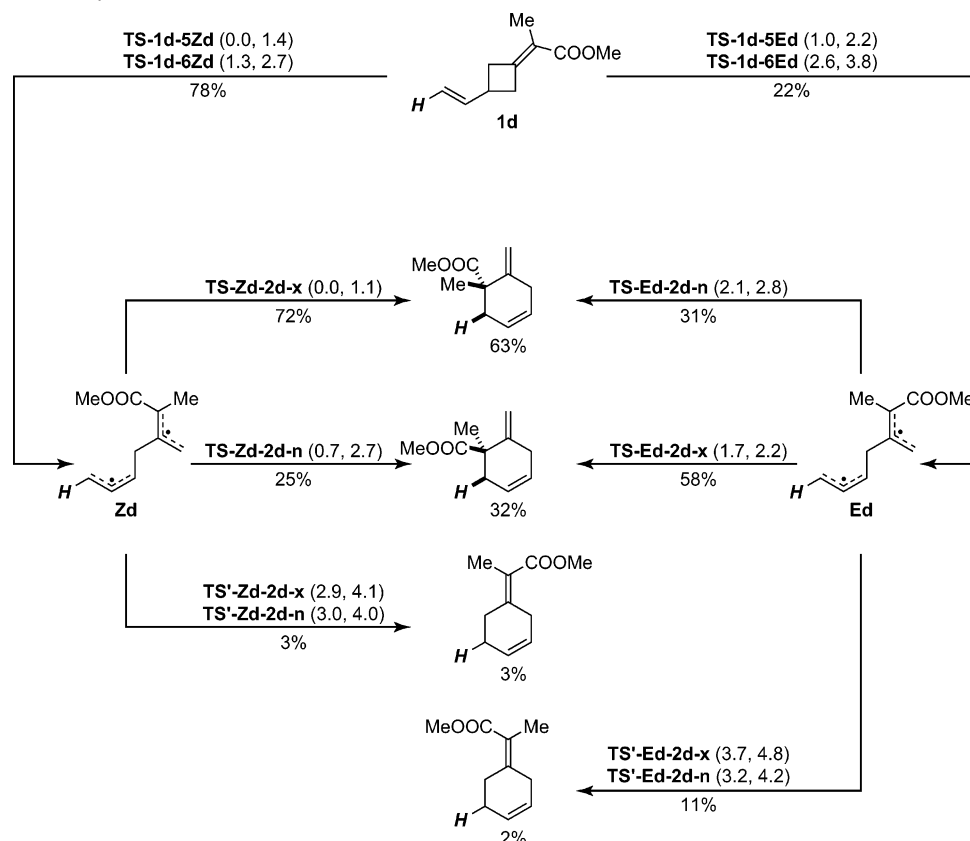


**Figure 9.** UB3LYP/6-31+G(d)-optimized *s-cis*-carbonyl ring-closing transition structures from the predominantly formed *Z* diradical intermediate. UB3LYP/6-31+G(d) enthalpies listed in kcal/mol relative to **TS-Zd-2d-x-cis**; enthalpies for corresponding *s-trans*-carbonyl structures are noted, although the structures are not shown (see Supporting Information).

structures, there appears to be unfavorable steric repulsion between Me and C4–H in their “*E*” counterparts.

**Ester and Methyl Group Effects on Bond Formation.** In the bond-forming step, calculations predict a regioselectivity opposite to that expected on the basis of product stability

**Scheme 4.** UB3LYP/6-31+G(d)-Predicted Product Selectivity in the Hypothetical Rearrangement of **1d** to **2d** under the Assumption of Complete Conformational Equilibration of Diradical Intermediates<sup>a</sup>



<sup>a</sup> Based on relative transition state enthalpies (in parentheses for each pair of *s*-cis- and *s*-trans-carbonyl isomers, respectively) in Figures 8, 9, and 10. “H” denotes the position of the *trans*-vinyl substituent, which is either a phenyl or methyl group in the Jung experimental system **1a/b**<sup>7</sup>.

(Figures 9 and 10). Despite the thermodynamic preference for forming the most-substituted double bond, the transition states that form a new  $\sigma$  bond to the Me/COOMe-substituted terminus (C7) are favored by 1.1–3.1 kcal/mol. This may be attributed to the fact that the radical-stabilizing Me and COOMe groups facilitate the necessary twisting of the C7 terminus out of conjugation with the C5–C6  $\pi$  system and into an orientation for bonding to C1 or simply to greater localization of the unpaired electron on C7 as opposed to C6. These substituent effects on the cyclization step, combined with the ring-opening selectivity discussed above, predict a preference for the [3s,3s] product, as shown in Scheme 4.

Scheme 4 gives calculated percentages of reactions in different stereochemical and regiochemical senses, as predicted for the (Me, COOMe)-substituted compound **1d**. These results show a significant preference for the overall stereochemistry found in the Jung experiments, where a phenyl or methyl group replaces the H in Scheme 4, and a trialkylsiloxy group resides at C3.

In the fully substituted Jung experimental system, the trialkylsiloxy group at C3 should shift the ring-opening preference toward **TS-1-6** rather than **TS-1-5**, as discussed as part of our piecewise analysis above. Although we have not attempted calculations with both sets of substituents at once, the preference for **TS-1-6Z** would be even further amplified by likely repulsive interactions between OSiR<sub>3</sub> and COOMe or Me in **TS-1-5Z** and **TS-1-5E**.

While we have not computed the entire system, the activation energy of the system studied experimentally can be approximated from the barriers for the model systems. Full-scale

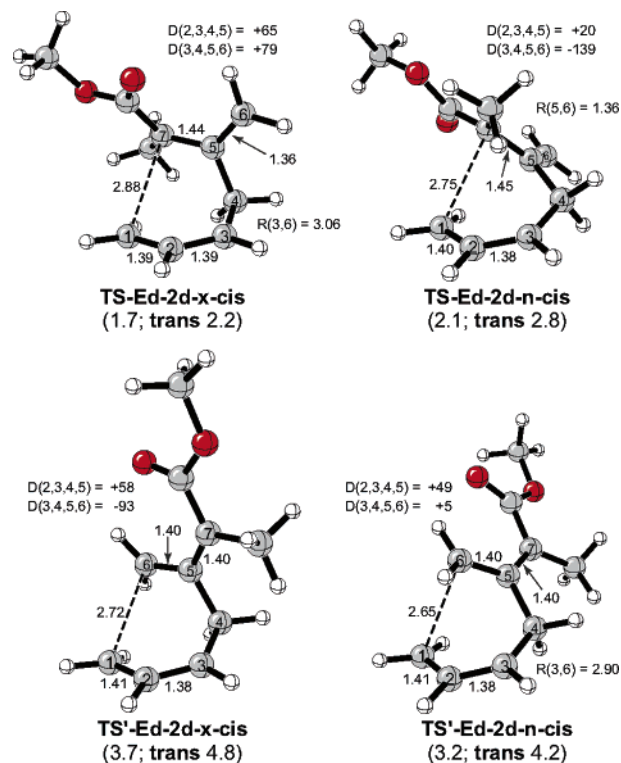


**Figure 10.** UB3LYP/6-31+G(d)-optimized *s*-cis-carbonyl ring-closing transition state structures from the lesser-formed, *E* diradical intermediate. UB3LYP/6-31+G(d) enthalpies listed in kcal/mol relative to **TS-Zd-2d-x-cis** (Figure 9); enthalpies for corresponding *s*-trans-carbonyl structures are noted, although the structures are not shown (see Supporting Information).

computation of these large systems was not feasible due to wave function convergence problems encountered with singlet-state optimizations. Therefore, the activation barriers were approximated by the homolysis energies, which were in turn approximated by optimizing diradicals in the triplet state and then performing single-point electronic energy calculations on those structures in the singlet state. This method provided a reasonable approximation to singlet-state optimization, as can be seen by comparing the energies of **6\*** and **6c\*** (computed as just described) to their singlet-optimized counterparts, **6** and **6c**. The full data are given in Table S1 of the Supporting Information. In this way, a lowering of the activation barrier by 7.5 kcal/mol versus the parent system was estimated. This is consistent with the facility of the reaction studied experimentally.

### Conclusion

The results for model systems suggest the following explanation of the overall selectivity observed in the rearrangement of **1a/b** to **2a/b**. The siloxy substitution enhances the formal Cope product by favoring a semi-direct **1** → **TS-1-6** → **6** → **TS-6-2-x** → [3*s*,3*s*]-**2** pathway. In contrast to the parent reaction,

siloxo substitution favors **TS-1-6** over **TS-1-5** in the first step of the reaction and it impedes randomization of the stereochemically rich intermediate **6** prior to cyclization to form the product. In addition, the ester and methyl substituents on the methylene group in **1** provide a strong preference for bond cleavage distal to the ester group, which contributes to the observed product stereochemistry. Finally, methyl/ester substitution in the diradical intermediate kinetically favors [3,3] regiochemistry in forming the new bond. These effects all conspire to cause a reaction that occurs by distinct bond cleavage and bond-formation events nevertheless to exhibit the high stereo- and regioselectivity that is usually the hallmark of concerted processes.

**Acknowledgment.** We thank the National Science Foundation for financial support of this research.

**Supporting Information Available:** Cartesian coordinates for all optimized structures; complete citations for refs 11, 12, and 13; and supplements to Figures 9 and 10. This material is available free of charge via the Internet at <http://pubs.acs.org>.

JA060913E